

# $\Lambda(1520)$ and $\Sigma(1385)$ resonance production in Au+Au and p+p collisions at RHIC ( $\sqrt{s_{NN}} = 200$ GeV)

Ludovic Gaudichet for the STAR collaboration ‡

E-mail: Ludovic.Gaudichet@subatech.in2p3.fr  
SUBATECH, École des Mines, 4 rue Alfred Kastler, 44307 Nantes, France

**Abstract.** The production of  $\Lambda(1520)$  in p+p and Au+Au collisions provided by the RHIC at  $\sqrt{s_{NN}} = 200$  GeV are investigated using the STAR detector. A preliminary  $\Sigma(1385)$  signal is also shown. Models predict that a late rescattering phase in ultra-relativistic heavy ion collisions should lower the measured yields of these resonances. This reduction is presently confirmed through the  $\Lambda(1520)/\Lambda$  ratio which has been calculated for p+p collisions and compared with Au+Au collisions.

PACS number: 25.75.Dw

## Introduction

Ultra-relativistic heavy ion collisions allow the study of created hot and dense matter. The produced system is thought to evolve into different stages before it breaks up. In particular an early partonic stage is followed by the hadronization of the system. An important rescattering phase may appear at the end of this scenario. It is of the utmost importance to understand these final steps of heavy ion collisions. Firstly because the study of this cooling medium will constrain our models of heavy ion collisions and secondly because most of our observations take their final shape during these phases. Therefore the existence of specific observables which are able to probe especially the hadronization and an eventual rescattering phase are of great interest. Resonances produced during the hadronization are such observables. Their short lifetime means that many of them decay inside the hot and dense medium before the system breaks up. Two types of effects are thought to appear. The reconstruction of resonance signal through the decay tracks reveals the properties of the resonance inside this medium. Mass modification or width broadening have been expected [2] and are reported by the STAR experiment [3]. The second effect probes the existence of particle rescattering in the hadronic gas. Since they are produced inside the medium, decay tracks may undergo rescattering with other particles and lose the momentum information on the decay. The yield of resonances could therefore be reduced. The momentum dependence of the rescattering may also modify the observed momentum distribution of resonances. In order to investigate this medium effect, the production of  $\Lambda(1520)$  and  $\Sigma(1385)$  in p+p and Au+Au collisions are presented at  $\sqrt{s_{NN}} = 200$  GeV, as measured by the STAR experiment. Models investigating the rescattering

‡ See [1] for the full collaboration list.

phase expect indeed both resonances to show a significant suppression in heavy ion collisions.

## 1. Models

### 1.1. Strange hadron resonances within a statistical model and rescattering effect

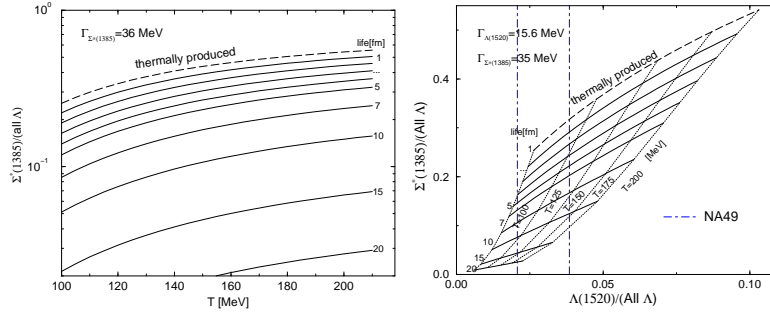


**Figure 1.** Left (a) :  $\Sigma(1385)/(All \Lambda)$  ratio as a function of the temperature at chemical freeze-out and the lifetime of the rescattering phase  $\Delta t$ . Right (b):  $\Sigma(1385)/(all \Lambda)$  versus  $\Lambda(1520)/(all \Lambda)$  diagram for different  $T$  and  $\Delta t$  ; (figures from [4])

Strange hadron resonances could determine the time scale governing hadron production and the duration of the decoupling phase. Ratios of yields of resonances over the ground state particles with the same valence quarks are estimated by a thermal model where the temperature is the only parameter. However the rescattering of decay products reduce the observed yields of resonances. This process can be taken into account by a microscopic model which calculates the suppression of the resonance signal during the hadronic phase. Thus coupling the thermal production and the rescattering characterization allows one to calculate these ratios as a function of the time between chemical and thermal freeze-out ( $\Delta t$ ) versus the temperature at chemical freeze-out  $T$  [5]. Figure 1 (a) shows the  $\Sigma(1385)/(All \Lambda)$  ratio as a function of the temperature and  $\Delta t$ . Figure 1 (b) demonstrates that using at least two resonances with different lifetimes gives a unique value for both  $T$  and  $\Delta t$ . However the model is not complete since it does not take into account the resonance regeneration by re-interaction of decay products in the hadronic gas.

### 1.2. Probing chemical and thermal freeze-outs via UrQMD

The microscopic transport approach of the Quantum Molecular Dynamics model (UrQMD) [6] can directly address the question of the production and observability of resonances [7]. Dynamics are described in terms of inelastic and (pseudo) elastic collision rates. After an early non equilibrium stage, the system is dominated by inelastic collisions and chemistry changing processes. The elastic and pseudo-elastic collisions become dominant in the next stage where they mostly change the momenta of the hadrons. The model shows therefore a separation between a chemical freeze-out and thermal freeze-out, i.e. a period of time when resonance signal can be destroyed. The lowering of the resonances observability can directly be calculated by dividing the

$$\begin{aligned} \Lambda(1520) &\rightarrow pK^- \quad (22.5\%) \\ \Sigma(1385)^- &\rightarrow \Lambda\pi^- \quad (88\%) \quad (\text{decay mode shared with the } \Xi^-) \\ \Sigma(1385)^+ &\rightarrow \Lambda\pi^+ \quad (88\%) \end{aligned}$$

**Table 1.** Observable decay channels in STAR for  $\Lambda(1520)$  and  $\Sigma(1385)$  resonances.

number of resonances for which decay products have survived the rescattering phase by the number of all produced resonances. It appears that 30% of  $\Lambda(1520)$  produced in UrQMD at  $\sqrt{s_{NN}} = 200$  GeV should not be observable due to the rescattering of at least one of the decay products. Part of this suppression comes from a double counting process. A resonance which decays and then is regenerated by a reaction involving one of its decay products is counted twice in the number of generated resonances but once in the number of suppressed resonances.

## 2. Data analysis

Table 1 shows the decay channels which are used in the reconstruction of  $\Lambda(1520)$  and  $\Sigma(1385)$ . The large Time Projecting Chamber (TPC) of STAR has been used to detect the charged tracks at mid-rapidity. Due to the short lifetime of these resonances, the secondary vertex of their decay can not be separated from the primary vertex of the collision. Signal reconstruction is therefore obtained by associating all selected tracks of the daughter species which seem to come from the primary interaction. Reconstruction of  $\Sigma(1385)$  is done via combinations of three tracks, the pion of the resonance decay and the two decay tracks of the reaction  $\Lambda \rightarrow p\pi^-$  (64%). The large combinatorial background is reproduced by event mixing [9]. Flow in heavy ion collisions or jet processes in p+p collisions introduce an azimuthal asymmetry to the analyzed events. This asymmetry leads to a characteristic shape on mixed event distributions. This behavior has been corrected for all invariant mass distributions of  $\Lambda(1520)$  [10].

Seven million minimum bias p+p events have been used to produce the  $\Sigma(1385)$  signal. The  $\Lambda(1520)$  analyses use 10 million p+p events, 1.7 million minimum bias Au+Au events and 1.7 million central trigger Au+Au events. Au+Au minimum bias events are divided in four centrality categories from peripheral to most central events : 80-60%, 60-40%, 40-10%, and 10% or less of the hadronic cross section.

## 3. Results

### 3.1. $\Lambda(1520)$ and $\Sigma(1385)$ in p+p collisions

Figure 2 shows separately the invariant mass distributions of  $\Lambda(1520)$  and  $\bar{\Lambda}(1520)$  in p+p collisions. The mass and width are respectively  $m = 1518 \pm 2$  MeV/ $c^2$  and  $\Gamma = 25 \pm 5$  MeV/ $c^2$  from a Breit-Wigner plus linear background fit. The mass agrees with the Particle Data Group value of  $1519.5 \pm 1$  MeV/ $c^2$  [11]. The experimental width includes the  $\Lambda(1520)$  natural width of  $15.6$  MeV/ $c^2$  and the momentum resolution. Within the errors this broadening of the width agrees to the Monte Carlo simulations of the  $\Lambda(1520)$  reconstruction. The raw ratio  $\bar{\Lambda}(1520)/\Lambda(1520)$  is equal to

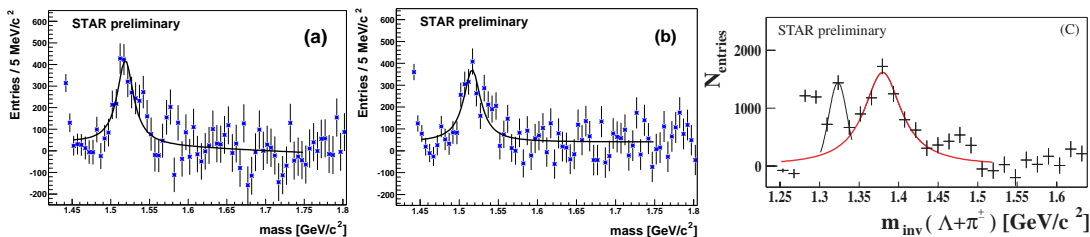


**Figure 2.** Invariant mass distribution of (a)  $\Lambda(1520)$ , (b)  $\bar{\Lambda}(1520)$  and (c)  $\Sigma(1385) + \bar{\Sigma}(1385)$  in  $p+p$  collisions.

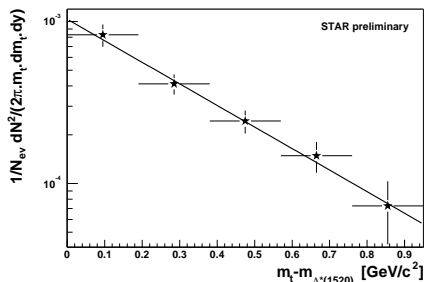


**Figure 3.** Transverse mass distribution of  $(\Lambda(1520) + \bar{\Lambda}(1520))/2$  for the  $p+p$  collisions. Errors shown are statistical only.

$0.90 \pm 0.11(stat)$ . Both  $\Lambda(1520)$  and  $\bar{\Lambda}(1520)$  signals have been added to decrease the statistical errors in the transverse mass distribution ( $m_T = \sqrt{P_T^2 + m_0^2}$ ) of figure 3. In order to correct raw yields, one Monte Carlo  $\Lambda(1520)$  has been embedded per real  $p+p$  event. The analysis procedure has then been applied on the simulated resonances to calculate the efficiency and acceptance of the detector. The corrected transverse mass distribution of  $(\Lambda(1520) + \bar{\Lambda}(1520))/2$  has been fit to an exponential function in order to extrapolate the  $dN/dy = 0.0039 \pm 0.0003(stat)$  and the slope parameter  $T = 326 \pm 42(stat)$  MeV. Systematic errors are determined by varying cuts, signal extraction and fit procedures. Systematic error on yield is 15% while the systematic error on the slope parameter is about 30%.

Preliminary invariant mass distribution of  $\Sigma(1385) + \bar{\Sigma}(1385)$  is shown in figure 2 (c). The left peak is due to the  $\Xi$  and  $\bar{\Xi}$  hyperons at the measured mass of  $1321 \pm 1$  MeV/c<sup>2</sup>. The right peak is fit to a Breit-Wigner plus a linear background function. The mass and width are  $m = 1381 \pm 2$  MeV/c<sup>2</sup> and  $\Gamma = 58 \pm 7$  MeV/c<sup>2</sup>. The integrated raw yield of  $\Sigma(1385) + \bar{\Sigma}(1385)$ , extracted from the fit, is about  $7500 \pm 100$  particles out of the 7 million minimum bias  $p+p$  events, with a 20% systematic error.

### 3.2. $\Lambda(1520)$ in $Au+Au$ collisions

The gold minimum bias data set shows a  $\Lambda(1520)$  signal for the two most peripheral categories. Figure 4 (a) and (b) shows the invariant mass distributions.  $\Lambda(1520)$  and  $\bar{\Lambda}(1520)$  signals are added to be more statistically significant. The 80-60% distribution has a three sigma signal while the 60-40% distribution shows a two sigma signal. Transverse mass distributions can not be performed due to the small

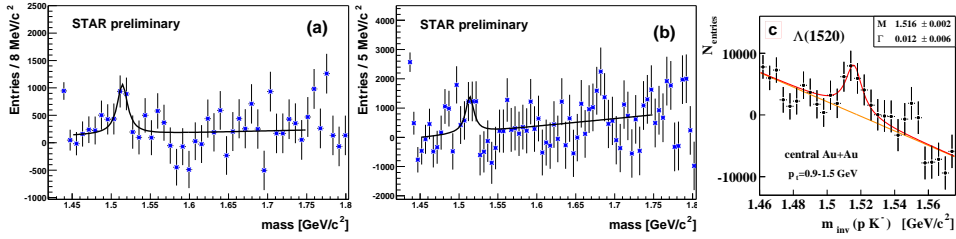


**Figure 4.**  $\Lambda(1520) + \bar{\Lambda}(1520)$  invariant mass for (a) the 80-60% and (b) the 60-40% centrality categories of minimum bias Au+Au events.  $\Lambda(1520)$  invariant mass distribution for the STAR central events (c).

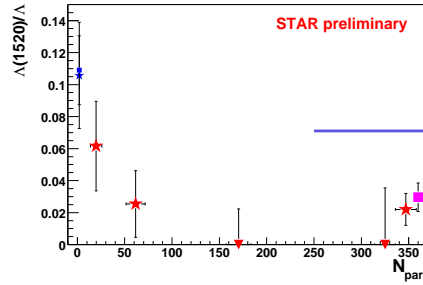


**Figure 5.** ratio  $\Lambda(1520)/\Lambda$  as a function of the number of participants and thermal prediction (line) from [14].

numbers of detected resonances. Integrated yields have therefore been calculated assuming exponential  $m_T$  distributions. Slope parameters, extracted from  $\Lambda$  analyses, are  $T = 260$  MeV for the 80-60% signal and  $T = 290$  MeV for the 60-40% signal.  $\Lambda(1520)$  and  $\bar{\Lambda}(1520)$  mid-rapidity production is  $0.086 \pm 0.039$  per unit of rapidity per event for the 80-60% category. The yield is  $0.12 \pm 0.1$  for the 60-40% category. Quoted errors include 30% systematic errors. Figure 4 (c) shows central collision measurement of the yield  $\langle \Lambda(1520) \rangle_{|y| < 0.5} = 0.58 \pm 0.021(\text{stat}) \pm 30\%(sys)$  [12].

### 3.3. $\Lambda(1520)/\Lambda$ ratios

In order to estimate the predicted reduction of  $\Lambda(1520)$  signal in heavy ion collisions, the ratio  $\Lambda(1520)/\Lambda$  has been calculated for Au+Au collisions at different centralities and is compared to the same ratio for p+p collisions. Figure 5 includes all  $\Lambda(1520)/\Lambda$  ratios as a function of the number of participants. Square points show NA49 ratios in p+p and Pb+Pb collisions at  $\sqrt{s} = 17$  GeV [13]. Other points are STAR measurements.  $\Lambda(1520)/\Lambda$  ratios from the two most peripheral categories of Au+Au collisions are represented at  $\langle N_{part} \rangle \sim 20$  and  $\langle N_{part} \rangle \sim 62$ . Arrows show upper limits at 95% of confidence level for more central categories of minimum bias events where no  $\Lambda(1520)$  signal is visible. A thermal prediction from [14] is also represented by the horizontal line. The ratio shows a significant decrease from p+p collisions to peripheral Au+Au collisions. Furthermore the production of  $\Lambda(1520)$  in heavy ion collisions is lower than the yield predicted by a thermal model.

## Summary

We report preliminary results on the production of  $\Lambda(1520)$  resonances in p+p collisions and in centrality categories of Au+Au heavy ion collisions at RHIC at 200 GeV.  $\Sigma(1385)$  signal is also shown in p+p collisions. The  $\Lambda(1520)/\Lambda$  ratio have been determined for the different systems. Results agree with NA49 data and show a decrease of the  $\Lambda(1520)$  yield relative to the  $\Lambda$  yield. Already lower than the p+p value in peripheral collisions, the  $\Lambda(1520)/\Lambda$  ratio appears to be significantly lower than the thermal expectation. These results are in qualitative agreement with model predictions of a lowering of resonance production in ultra-relativistic heavy ion collisions, due to the rescattering of decay products in the medium.

## Acknowledgments

I would like to thank Christina Markert and Sevil Salur for their contributions to this work and Patricia Fachini for helpful discussions. STAR acknowledgements can also be found in [1].

## References

- [1] H. Caines, these proceedings.
- [2] E.V. Shuryak and G.E. Brown, Nucl. Phys. A717:322-335 (2003) .
- [3] P. Fachini, these proceedings.
- [4] C. Markert, G. Torrieri, J. Rafelski, hep-ph0206260.
- [5] G. Torrieri and J. Rafelski, Phys. Lett. B509:239-245 (2001).
- [6] M. Bleicher, E. Zabrodin, C. Spieles, S.A. Bass, C. Ernst, S. Soff, L. Bravina, M. Belkacem, H. Weber, H. Stöcker, W. Greiner, J. Phys. G 25:1859 (1999).
- [7] M. Bleicher and J. Aichelin, Phys. Lett. B530:81-87 (2002).
- [8] M. Bleicher, private communication.
- [9] Drijard D et al, Nucl. Instrum. Methods A225:367 (1984).
- [10] L. Gaudichet, STAR note SN446.
- [11] Particle Data Group, Eur. Phys. J. C3 (1998).
- [12] C. Markert, proceedings of the 19th Winter Workshop on Nuclear Dynamics, Breckenridge.
- [13] V. Friese for the NA49 Collaboration, Nucl. Phys. A698:487-490 (2002).
- [14] P. Braun-Munzinger et al, PLB 518:41 (2001) ; D. Magestro, private communication.